Effect of non-mesogenic chiral terphenylate on the formulation of room temperature ferroelectric liquid crystal mixtures suitable for display applications

Asim Debnath[1], Pradip Kumar Mandal[1*], Abhisakh Sarma[2], and Olof Gutowski[2]

[1]Department of Physics, University of North Bengal, Siliguri, India-734013

[2]Deutches Electronen-Synchrotron DESY, 22607 Hamburg, Germany

* Corresponding author. Email address: mandalpk.phys@nbu.ac.in

Abstract: By varying the concentration of a chiral terphenylate dopant in a four-component achiral phenyl pyrimidine-based host mixture we have formulated six ferroelectric liquid crystal mixtures. Though the dopant is non-mesogenic it is observed that only 2wt% of it induces polarity in the host mixture at 32°C. With increasing concentration, the mixtures show ferroelectric behaviour even below ambient temperature down to at least 12°C. Optical polarizing microscopy, differential scanning calorimetry, dielectric and electro-optic studies reveal that with respect to temperature range, phase sequence, spontaneous polarization, optical tilt angle and switching time the formulated mixtures are suitable for ferroelectric based liquid crystal displays.

Keywords: room temperature ferroelectric mixture; optical tilt; X-ray tilt; spontaneous polarization; switching time

1. Introduction

A material is said to be ferroelectric if it possesses a spontaneous polarization in absence of an external field and if its polarization is switched between +ve and –ve states when the applied electric field is reversed. In general, some special types of solid materials which have non-centrosymmetric space group show ferroelectricity [1,2]. But, way back in 1974, using elegant symmetry considerations, Robert Meyer showed that ferroelectric properties could also be exhibited by fluid materials like tilted smectic liquid crystals if composed of chiral polar molecules [3,4]. Due to the reduced symmetry, SmC* phase possesses a spontaneous polarization (P_S) in absence of an external electric field and on the application of an electric field the molecules switch around an imaginary cone such that the sign of the P_S gets reversed. The sign of the P_S can again be reversed to the initial state when an electric field of opposite direction is applied. Such type of switching of the molecules from one orientation to another in presence of electric field simultaneously changes the optical effect of the materials and mainly this electro-optical effect is employed in ferroelectric liquid crystal based display devices. With the help of this switching mechanism, Clark and Lagerwall first reported an ferroelectric display device which is known as surface stabilized ferroelectric liquid crystal (SSFLC) display device [5]. Subsequent interest in this field has increased tremendously in the last few decades. Several parameters such as temperature range, switching time, spontaneous polarization, tilt angle, length of the pitch, viscosity, etc are important characteristics of such materials. In order to achieve the desired properties of a display device one has to optimize all these parameters. But a single compound cannot satisfy all such requirements and hence multi-component liquid crystal mixtures are usually formulated to optimize all the required properties necessary for display applications. Generally, a multi-component mixture consists of two main constituents viz, achiral host mixture and a chiral dopant. The host mixture is usually a mixture of several achiral compounds with a reasonably wide SmC phase temperature range starting from room temperature or below, which controls the overall temperature range and tilt angle of the final mixture. On the other hand, the dopant is a compound with one or two chiral centers which controls the spontaneous polarization, viscosity, switching speed and the helical pitch of the final mixture [6-10]. Keeping all these things in mind we have prepared a four-component pyrimidine-based achiral host mixture (**HM**) which after doping with a non-mesogenic chiral dopant (**NMC**) resulted in several room temperature ferroelectric liquid crystal mixtures.

In this article, we report how the concentration of the **NMC** dopant influences the mesophase behaviour and the physical properties critically important for electro-optical properties of the display devices. It is observed that when only 2wt% of **NMC** dopant is added to the **HM** it induces SmC* phase at about 32^{o}C and with increased concentration it exhibits SmC* phase below ambient temperature down to at least 12°C. These mixtures are found to possess high spontaneous polarization and relatively fast switching time which can be used in liquid crystal display devices.

2. Experimental Techniques

For the preparation of the host mixture **HM** we used four achiral phenyl pyrimidine compounds having tilted SmC phase. Molecular structures, transition temperatures and composition of the mixing components are shown in **Table 1**. Dopant **NMC** is a non-mesogenic protonated chiral terphenyl compound with chiral centres at opposite ends and it has a high melting point (79.4^{o}C). Molecular structure and transition temperature of the dopant are shown in **Table 2**. Final mixtures were prepared by adding various wt% of the **NMC** dopant in the host mixture (**HM**). To make them homogeneous the above mixtures were dissolved in chloroform and ultrasonicated at 65°C until evaporation of chloroform was completed.

Table 1. Molecular structures and transition temperatures of the components and phase sequence of the host mixture

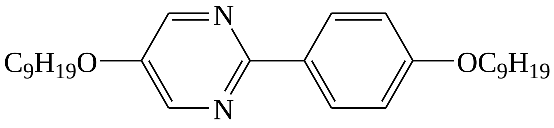

H1: Cr 61.8ºC SmC 95.6ºC SmA 99.1ºC I

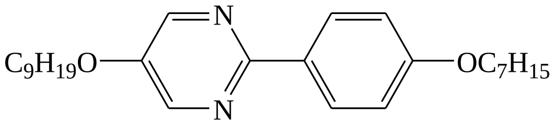

H2: Cr 57.4ºC SmC 95.1ºC SmA 98.4ºC I

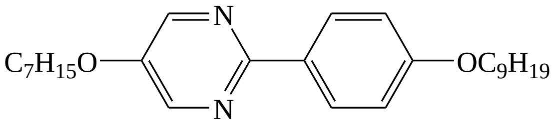

H3: Cr 57.2ºC SmC 79.1ºC SmA 91.2ºC N 94.7ºC I

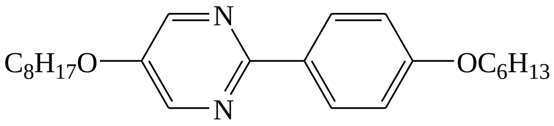

H4: Cr 27.5ºC SmC 46.3ºC SmA 57.5ºC N 65.6ºC I

Host Mixture (**HM**)

Composition (wt%)	Phase sequences and transition temperatures
H1: **H2 : H3 : H4 ::** 20 : 20 : 20 : 40	Cr 19°C SmC 69.4°C SmA 78.7°C N 81.2°C I

Table 2. Molecular structure and transition temperature (ºC) of the **NMC** dopant

Sample	Molecular structure and transition temperature
NMC	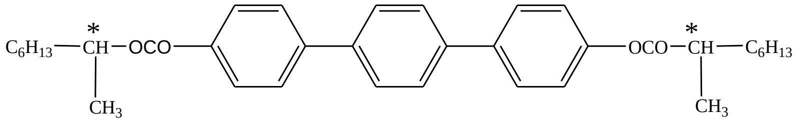 Cr 79.4 Iso

Polyimide-coated homogeneous (HG) dielectric cells, made of low resistive (about 10Ω/sq.) transparent indium tin oxide (ITO) coated electrodes having an effective area of 1 cm^2 and a cell gap of 5 µm, were used for optical polarizing microscopy, dielectric, electro-optic, and synchrotron diffraction study. Cells were filled by capillary action with samples in isotropic state and to get proper alignment of the samples within the cell very slow regulated cooling was made.

Phase behavior and transition temperatures of the compounds and their mixtures were investigated by studying their topological defect structures (textures) under an Olympus BX41 polarizing microscope (OPM) equipped with a CCD camera. Using a Mettler FP90 temperature controller and FP82HT hot stage temperature of the samples was regulated with an accuracy of ±0.1°C. All the observations were made during heating at the rate of 0.2^{o}C/min. Phase transition temperatures had also been determined by differential scanning calorimeter (DSC) using the same temperature controller but with different hot stage FP84HT and the FP99A software. During DSC measurements heating rate was taken as 5^{o}/min.

Structural investigation of the phases was made using PETRA III synchrotron beamline P07 at Physics Hutch station (EH2) at DESY, Hamburg. Synchrotron beam of wavelength $\lambda = 0.2483$ Å was used and angular range (2θ) of nearly 0-3^{o} was covered. To avoid large absorption by the glass plates of the cell in normal geometry, the synchrotron beam was made to pass through the 5 μm cell gap keeping parallel to the cell surfaces. A Perkin Elmer 2D detector was used for data collection. The total size of the detector was 400×400 mm^2 with individual pixel size 200×200 μm^2 and it was placed 3.3 m away from the sample. QXRD program of G Jennings (version 0.9.8, 64 bit) was used for data acquisition. The same program was also used for analyzing the images. Images were integrated using a step size of 0.001° to get the diffraction patterns (intensity versus Bragg angle 2θ). In this experiment, cell temperature was regulated with a LakeShore 340 temperature controller. Layer spacings were calculated using Bragg's relation; the peak positions were determined by fitting a Lorentzian function to intensity profile data.

Complex dielectric permittivity of the mixtures was measured using a Hioki 3532 50 impedance analyzer in the frequency range from 50 Hz to 5 MHz, and automatic data acquisition arrangement was made using RS 232 interfacing with a PC.

Spontaneous polarization (P_S) was measured as a function of temperature by the reversal current method [11] using a triangular wave (5-70 Vpp, 10 Hz) obtained from an Agilent 3320A function generator. A digital storage oscilloscope (Tektronix TDS 2012B) was used to record the voltage drop (V) across a resistor (R) in series with the cell as a function of time. The area under the curve was determined from the stored image after creating an appropriate baseline using commercial software. P_S was calculated using the expression

$$P_S = \frac{\int V dt}{2AR} \qquad \textbf{(1)}$$

where A is the active area of the cell.

Measured P_S data were fitted to the mean-field equation [12]

$$P_S = P_0(1 - T/T_C)^{\beta} \qquad \textbf{(2)}$$

to extract the value of the critical exponent (β) for the secondary order parameter P_S and the SmC*-SmA* transition temperature (T_C).

Tilt angle (θ), the angle made by the molecular long axis with the layer normal is the primary order parameter of ferroelectric SmC* phase while P_S is the secondary order parameter which is an outcome of the tilt. In this study, tilt angle θ was measured by electro-optical (θ_{opt}) method as well as by X-ray ($\theta_{X\text{-}ray}$) diffraction technique. On the application of an external ac field the molecules switch around an imaginary cone through twice the tilt angle (2θ) thereby reversing the sign of the spontaneous polarization. So the tilt of the molecules in smectic layers (θ_{opt}) was determined by measuring the angle of rotation of the FLC cell between two extinction conditions viewed between crossed polarisers under a microscope while observing switching of the molecules under a square pulse (magnitude 20-60 V_{pp}) of very low frequency (10 mHz) [13]. On the other hand, the X-ray tilt was calculated from the measured layer spacings using the relation

$$\theta_{X-ray} = \cos^{-1}\left(\frac{d_C}{d_A^{\max}}\right) \quad \textbf{(3)}$$

where d_C is the layer spacing in SmC* phase and d_A^{max} is the maximum layer spacing observed in SmA* phase.

Response time was also measured by observing the switching of the molecules under a square pulse in the same dielectric cell. When a square wave pulse (20-60 Vpp, 10 Hz) was applied to the cell, a polarization bump occurred away on the time scale from the square pulse edge of the applied voltage. Measurement of the delay in the time provided the response time (τ) of the sample. For accurate measurement of τ, oscilloscope data were stored in a computer and were analyzed by commercial software.

Rotational viscosities of the mixtures were calculated from the measured P_S and τ using the relation [14]

$$\gamma_\varphi = \tau P_S E \quad \textbf{(4)}$$

where E was the applied electric field.

Estimated errors in optical tilt angle, spontaneous polarization and response time measurements were found to be nearly ±0.1°, ±0.5 nC/cm^2 and ±1 µs, respectively.

Table 3. Composition, phase sequences, transition temperatures (°C) and thermal range of SmC* phase (ΔT) of the mixtures obtained from OPM and DSC studies. Transition temperatures from DSC are shown within parentheses.

Mixture	Composition (wt%)	Transition temperatures	ΔT (°)
M1	**HM : NMC** :: 98 : 2	Cr 32.0 SmC* 88 SmA* 96.2 N* 97 I (30.9) (87.3) (95.7) (99.6)	56
M2	**HM : NMC ::** 95 : 5	Cr <12 SmC* 87.8 SmA* 95.8 N* 96.3 I (88.8) (94.3) (97.8)	70.8
M3	**HM : NMC ::** 90 : 10	Cr <12 SmC* 87.5 SmA* 95.0 I (88.4) (95.8)	70.5
M4	**HM : NMC ::** 85 : 15	Cr <12 SmC* 87.4 SmA* 93.7 I (88.1) (94.4)	70.4
M5	**HM : NMC ::** 80 : 20	Cr <12 SmC* 86.3 SmA* 91.8 I (86.7) (91.9)	70.3
M6	**HM : NMC ::** 75 : 25	Cr <12 SmC* 85.6 SmA* 90.6 I (85.8) (89.7)	68.6

3. Results and Discussions

3.1 OPM and DSC Study

Phase behavior and transition temperatures observed from OPM as well as from DSC study during the heating cycle are shown in **Table 3.** Phase diagram and the DSC thermograms of the mixtures showing the variation of heat flow with temperature are shown in **Fig. 1(a-c)**. It is observed that though the **NMC** itself is a non-mesogenic compound with a high melting point but when only 2 wt% of it was doped in the **HM** it induced polarity (mixture **M1)** and exhibited ferroelectric SmC* phase close to room temperature (~32 °C). In addition to SmC* phase, the mixture **M1** was also found to exhibit SmA* and N* phases before going to isotropic phase. At higher doping concentrations, the mixtures (**M2-M6**) exhibited SmC* phase below ambient temperature down to at least 12°C (below which we could not measure). It was also noticed that with the increase of doping concentration, the SmC*- SmA* transition temperature decreased slightly (that is the thermal range of the SmC* phase decreased) and the cholesteric phase disappeared above 5 wt% of **NMC**.

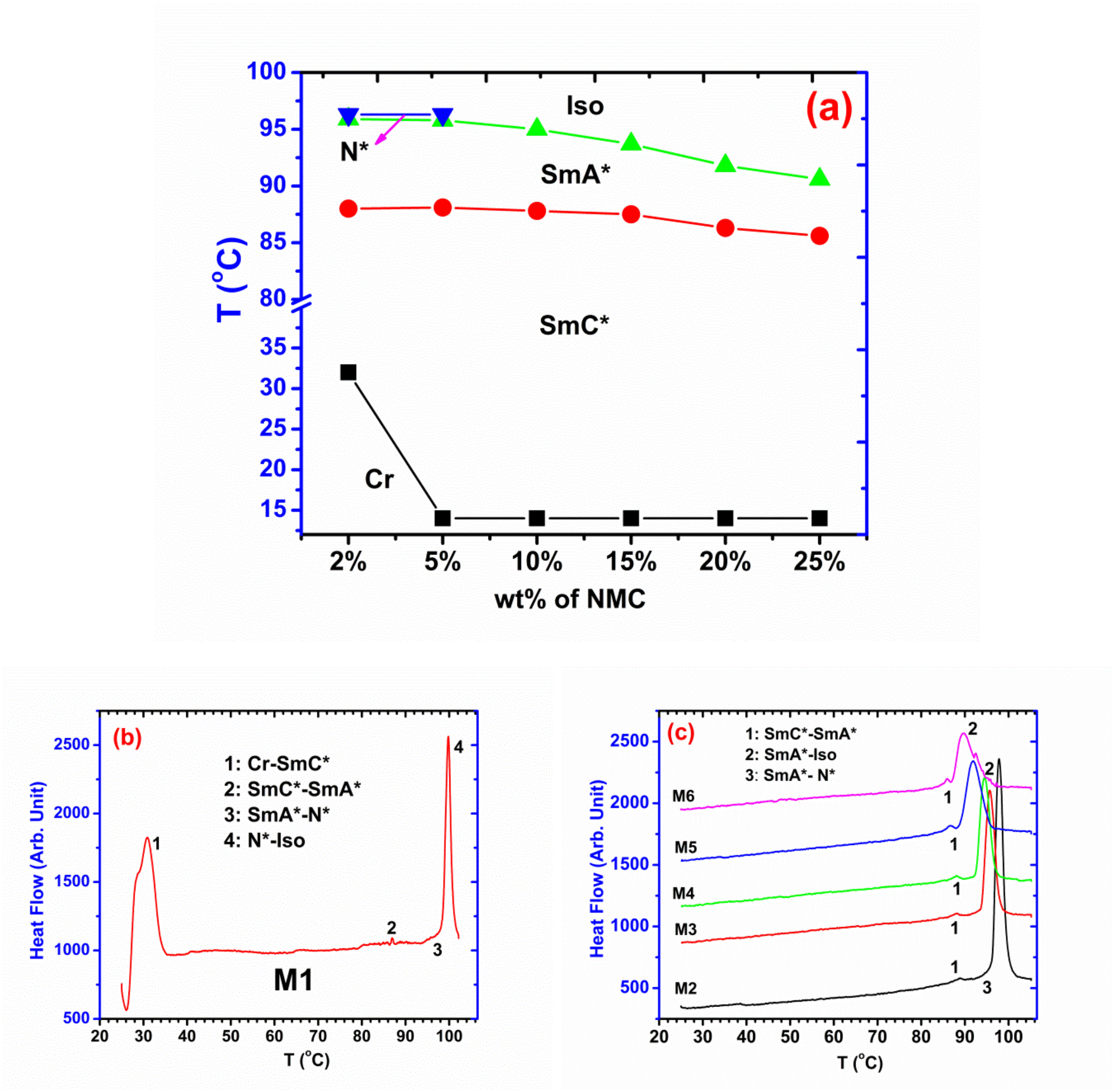

Fig. 1: (a) Phase diagram of the mixtures; DSC thermograms of (b) **M1** and **(c) M2**, **M3**, **M4**, **M5** and **M6** during the heating cycle at 5°C/min

As a representative example, textures of the mixture **M1** obtained under planar anchoring condition are shown in **Fig. 2(a-c)**. Typical domain texture was observed in SmC* phase which transformed into a uniform planar aligned texture in SmA* phase to a usual long pitch cholesteric droplets texture in N* phase before going to isotropic phase [15].

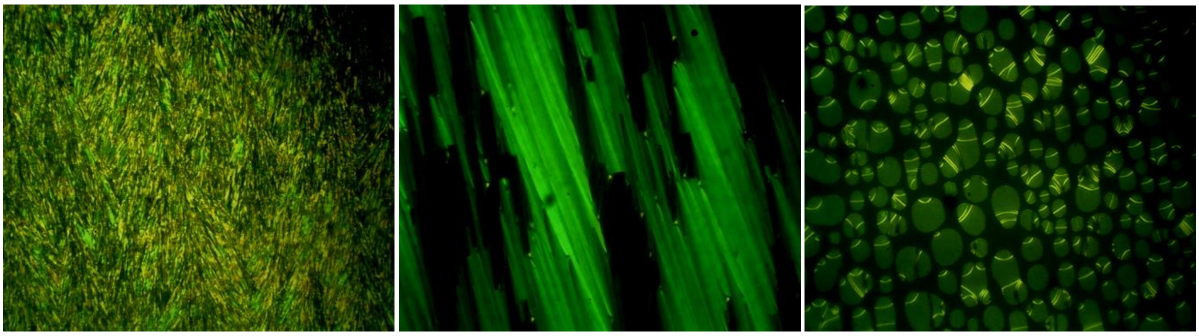

(a) SmC* (35°C) (b) SmA* (90°C) (c) N* (96.5°C)

Fig. 2: Observed textures of the mixture **M1**

It might be mentioned here that when four fluorinated chiral dopants differing only in number and location of fluorine atoms in the molecular rigid core were doped (60 wt% of each) in the same host mixture (**HM**) they produced two ferroelectric and two antiferroelectric liquid crystal mixtures [16,17]. Not only that, one of the dopant at lower concentration (10 wt%) produced an electroclinic mixture with large field-induced tilt and very small layer contraction [18] and at much higher concentration (75 wt%), it formed a wide range ferroelectric mixture with a few hundred micro-second switching time [19]. Also, a different fluorinated chiral dopant with an oligomethylene spacer was found to produce a ferroelectric mixture with much faster response time [20]. Even a binary mixture of one protonated oligomethylene spacer based chiral compound and one achiral biphenyl pyrimidine compound was found to exhibit room temperature ferroelectric mixture with moderate spontaneous polarization and sub-millisecond switching time [21]. Therefore, it might be inferred that the nature and concentration of the host and dopant influence the phase behavior and properties of the resulting mixtures enormously.

3.2 Synchrotron Diffraction Study

Mesophase structural investigation and temperature evolution of different phases of the mixtures were studied by synchrotron diffraction study. Transition temperatures were seen to be shifted to a higher temperature by 1-2^o than those observed from OPM and DSC study which probably resulted due to the use of different temperature baths. Very slow regulated cooling and planar polyimide coating of the inner surfaces of the cell resulted in an oriented sample. As shown in **Fig. 3(a)**, in SmC* phase, one very sharp low diffraction angle ring was observed characterizing one-dimensional positional ordering across the smectic layers. The sharpness of the ring slightly decreased in SmA* phase and finally converted into a diffused ring in N* phase **(Fig. 3(b-c))**. Temperature dependence of the layer spacings in smectic phases is shown in **Fig. 4.** It is observed that layer spacing in the SmC* phase increases with increasing doping concentration. Layer spacings of the mixtures are also found to be almost linearly additive approaching towards the most extended length of the **NMC** (32.41Å) obtained from the optimized geometry. From the figure, it is also noticed that the layer spacings increase with temperature, more in low concentration mixtures, signifying decrease of tilt angles of the molecules with respect to the layer normal which has been discussed further in **Section 3.5**.

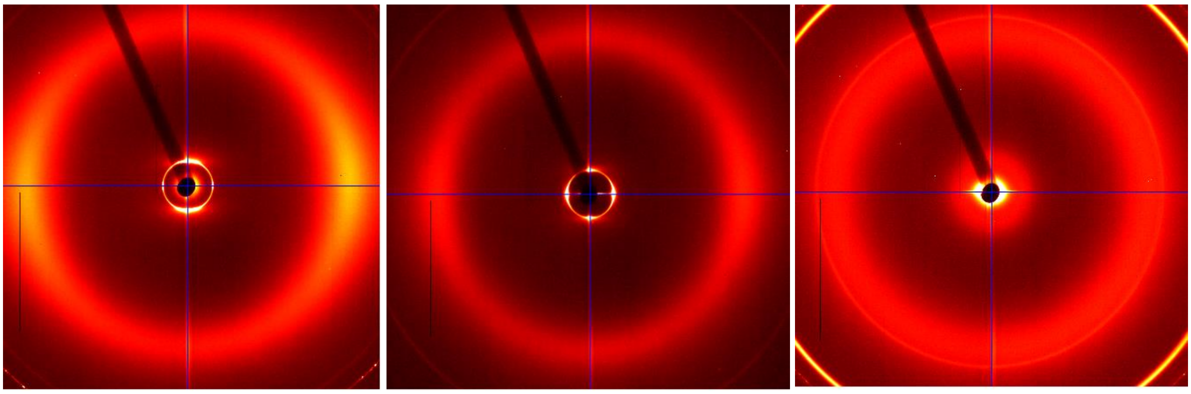

(a) SmC* (b) SmA* (c) N*

Fig. 3: Observed X-ray diffraction patterns of the mixture **M2**

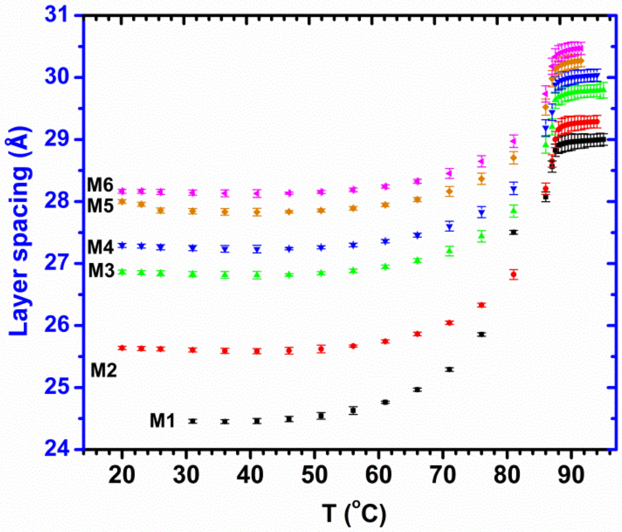

Fig. 4: Temperature variation of layer spacings of the mixtures**.**

3.3 Dielectric Permittivity Study

Transverse component of the real part of dielectric permittivity (ε′) in different phases for all the mixtures measured at 1 kHz as a function of temperature are shown in **Fig. 5**. The dielectric behaviour of the three liquid crystalline phases, viz. N*, SmA* and SmC* can be clearly distinguished on the basis of the magnitude of ε′. Except in the mixtures **M1**, **M2,** and **M3,** it has a very high magnitude in SmC* phase (~4 for **M1**, ~5 for **M2**, ~9 for **M3**, ~18 for **M4**, ~45 for **M5**, ~80 for **M6**). Thus it is seen that the increase of doping concentration increases the magnitude of the real part of dielectric permittivity rapidly which is due to the increased polarity of the resulting mixture. The temperature dependence of ε′ is also slightly different in the SmC* phase. In **M1** it decreases, in **M2** it remains almost constant, in **M3** and **M4** it slightly increases and in **M5** and **M6** it slightly increases initially, then decreases. However, in all the mixtures near the SmC*-SmA* transition temperature, ε′ shows a diverging trend and on further heating, it abruptly falls to a value of ~3 in SmA* phase. In **M1** and **M2**, the magnitude of ε′ of N* phase is found to be slightly higher than that of SmA* phase and shows a linearly increasing trend (~2.9-3.4 for **M1** and

~3.0-3.5 for **M2**) with temperature before going to the isotropic phase where it remains constant.

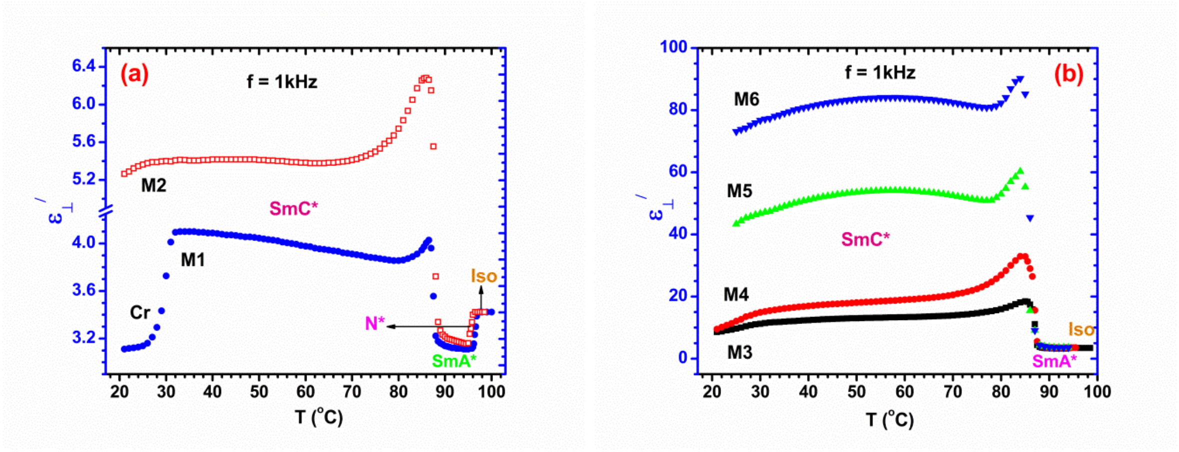

Fig. 5: Temperature variation of the real part of the dielectric permittivity (ε′): (a) **M1**, **M2** and **(b) M3**, **M4**, **M5** and **M6**

3.4 Spontaneous Polarisation (P_S) Study

To test the growth of P_S with the electric field it was measured as a function of the electric field at 20°C (only for **M1** at T = 32°C). From this measurement, we calculated the saturation electric field (E_{sat}), the field at which P_S become 90% of its maximum. It is seen from **Fig. 6(a-c)** that the E_{sat} values for the mixtures **M1-M6** are 12.5, 6.4, 5.2, 4.4, 4.2 and 4.0 V/μm, respectively. Thus the E_{sat} values are found to decrease with doping concentration which may be due to the fact that with increased concentration polarity of the mixtures increases and hence less electric field is required to align the dipoles.

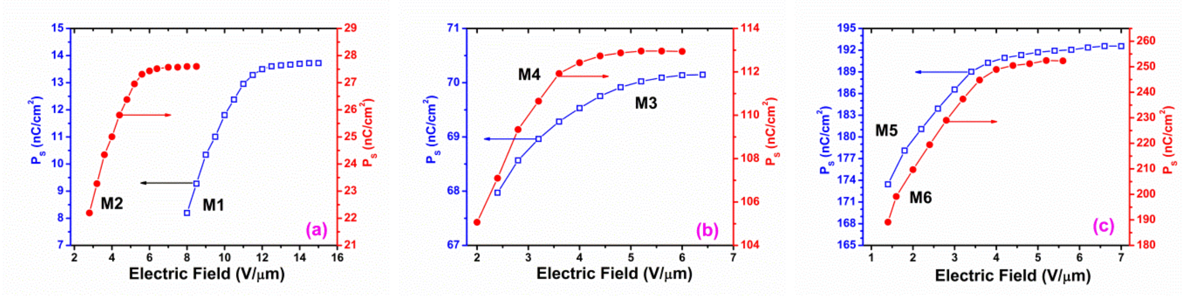

Fig. 6: Variation of spontaneous polarisation (P_S) with electric field: (a) **M1**, **M2**; (b) **M3, M4** and (c) **M5**, **M6**

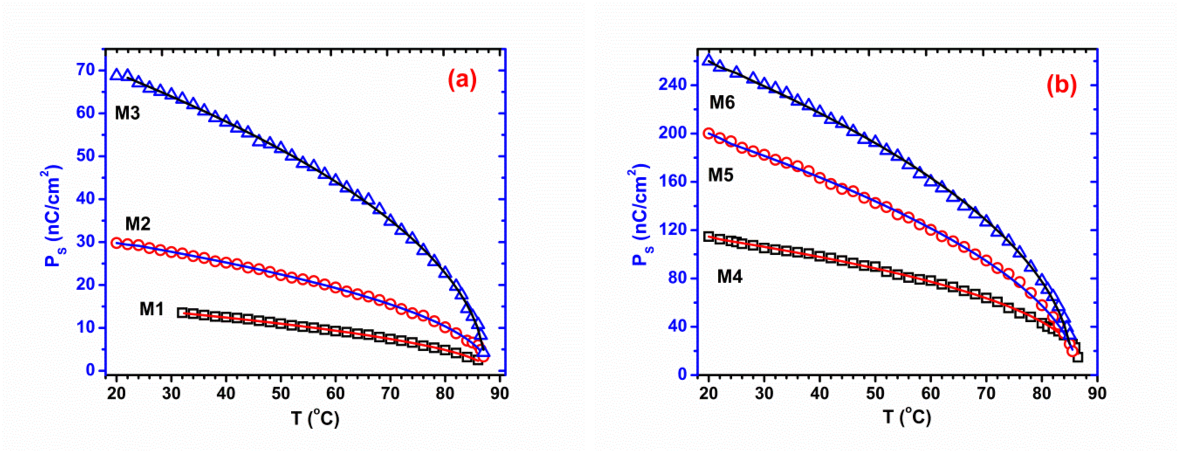

Fig. 7: Temperature variation of spontaneous polarisation (P_S): (a) **M1**, **M2**, **M3** and **(b) M4**, **M5,** and **M6**. Mean field fitted curves are shown as solid lines.

Temperature dependence of spontaneous polarisations (P_S) measured at E_{sat} is presented in **Fig. 7**. It is observed that the nature of variation of P_S with temperature is similar for all the mixtures, Ps decreases with increasing temperature as expected. But with doping concentration, P_S increases almost linearly: maximum values of P_S in the mixtures **M1** to **M6** are found to be about 14, 30, 70, 120, 200 and 260 nC/cm^2, respectively. Thus low dopant concentration induces less polarity in the mixtures compared to the higher dopant concentration as was revealed in the dielectric study. From the application point of view, moderate values of P_S (about 50-150 nC/cm^2) are required because high values of P_S build up a large internal field in the devices that make polarisation reversal difficult and low values of P_S require high electric field for reorientation, both of which are undesirable [22]. Thus so far P_S is concerned moderate concentration mixtures (10-15 %) are more effective.

P_S data are found to fit nicely to the mean-field model; the fitted parameters are listed in **Table 4**. From the table, one observes that the fitted T_C values are very close to the actual T_C and fitted β values are close to the critical exponent value (0.5) for a second-order phase transition according to mean-field model [23]. It seems that the nature of the SmC*-SmA* transition is second order. Very small enthalpy change observed in DSC study even at the heating rate of 5°/min is an indication of this type of phase change. However, discontinuous change in tilt angle, more prominent in optical tilt (discussed in the next section), does not support this observation.

Table 4. Comparison of fitting parameters of P_S

Mixture	Fitted T_C (°C)	Actual T_C (°C)	β (Critical exponent)
M1	88.02 ± 0.21	88.0	0.520 ± 0.006
M2	88.11 ± 0.13	87.8	0.500 ± 0.005
M3	87.36 ± 0.07	87.5	0.502 ± 0.003
M4	87.37 ± 0.13	87.4	0.482 ± 0.005
M5	86.48 ± 0.11	87.3	0.530 ± 0.005
M6	85.61 ± 0.16	85.6	0.492 ± 0.002

3.5 Tilt Angle (θ) Study

The tilt angle of the molecules determined by electro-optical and X-ray scattering methods are presented in **Fig. 8** and **Fig. 9**. The figures show that the general behavior of the tilt angle with temperature is the same for all the mixtures. An increase of the amount of the dopant **NMC** causes a decrease in the magnitude of the tilt of the mixtures. This decrease in primary order parameter (tilt angle) was also reflected in the thermal range of the SmC* phase which was confirmed by OPM and DSC study, as the dopant concentration increased SmC*-SmA* transition temperature decreased (see **Table 4** and **Fig. 1**). However, the maximum values of the optical tilt angles for the mixtures **M1** to **M6** are found to be about 34°, 30°, 26°, 25°, 23.5° and 22.5°, respectively. Optical tilt being close to 22.5°, the higher concentration mixtures (**M5** and **M6**) are, therefore, expected to be suitable for SSFLCDs [22]. They also show relatively less temperature dependence which means contrast and brightness of the display devices will be less temperature dependent.

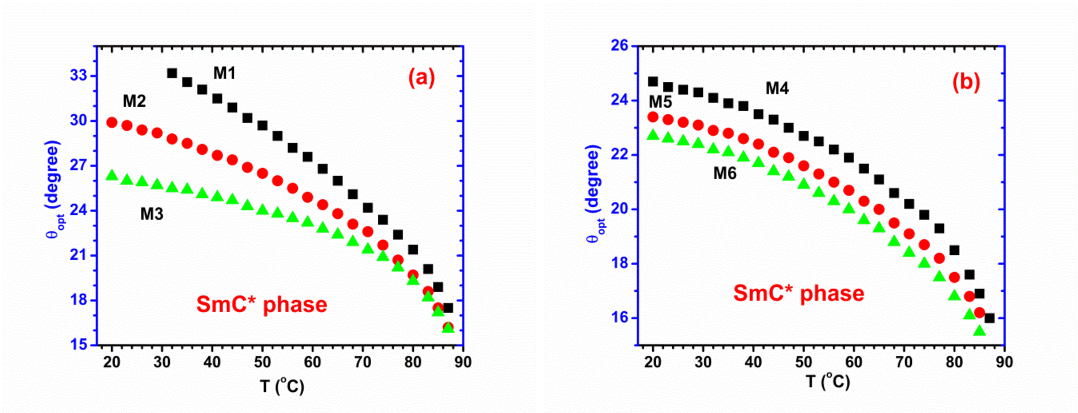

Fig. 8: Temperature variation of the optical tilt angle (θ_{opt}): (a) **M1**, **M2**, **M3** and **(b) M4**, **M5,** and **M6**

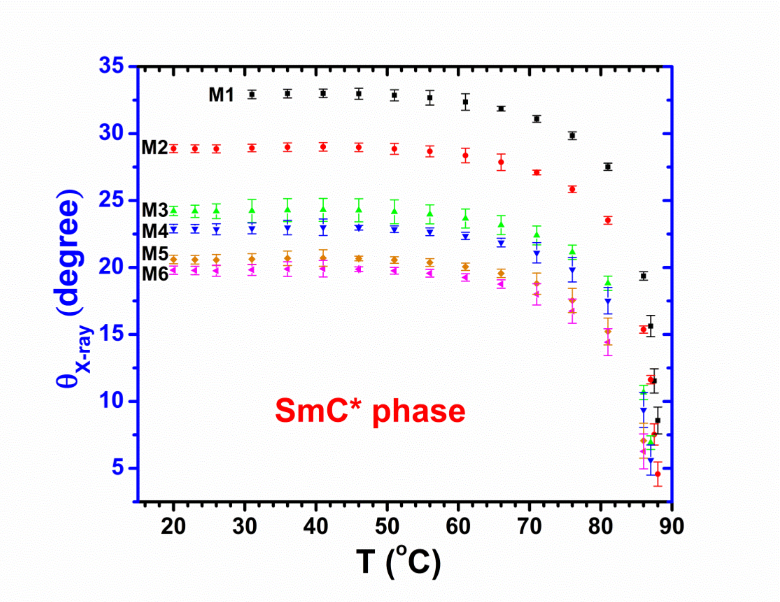

Fig. 9: Temperature variation of the X-ray tilt angle ($\theta_{X\text{-}ray}$) of the mixtures in SmC* phase

It is further noticed that although both the X-ray tilt ($\theta_{X\text{-}ray}$) and optical tilt (θ_{opt}) show similar temperature dependence, but X-ray tilt is slightly smaller than the optical tilt. This is because X-ray tilt is a result of the tilt of electron density function of the whole molecule whereas optical tilt arises due to the tilt of only the rigid polarisable group of the molecule. Since the host and the dopant molecules possess large flexible parts, X-ray tilt may be less than the optical tilt [24,25]. However, θ_{opt} is more useful from the application point of view.

3.6 Response Time (τ) Study

Observed temperature dependence of the response time of the mixtures is shown in **Fig. 10**. From the figure it is clear that all the mixtures show a similar type of temperature dependence, in low-temperature region τ decreases very quickly, then the rate of decrement falls off and finally, at high temperatures, it becomes almost constant. It is further observed that the magnitude of τ decreases with doping concentration: the maximum value of τ in the mixtures **M1** to **M6** being 680, 610, 550, 460, 340 and 260μs, respectively. Lower response time is desired from the application point of view because lower is the response time faster will be the electro-optical response of the device. Therefore, with respect to the response speeds higher dopant concentration mixtures (**M5** and **M6**) are suitable.

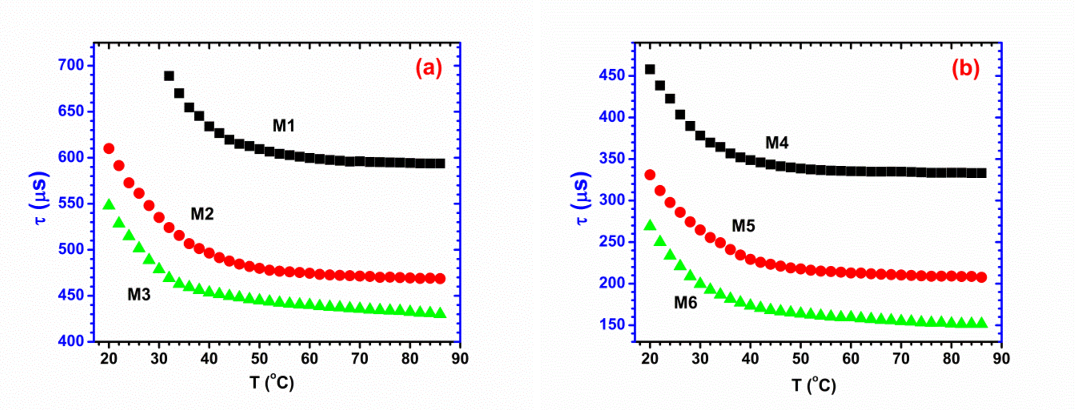

Fig. 10: Temperature variation of response time (τ): (a) **M1**, **M2**, **M3** and **(b) M4**, **M5,** and **M6**

3.7 Rotational Viscosity (γ_φ) and Activation Energy (E_a) Study

The rotational viscosity (γ_φ), related to the rotations of the molecules about the Smectic C cone, is an important parameter of the SmC* phase, which strongly influences the switching time between the field-induced states of FLCs.Temperature dependence of γ_φ is presented in **Fig. 11**. Rotational viscosity is found to increase linearly with concentration. In all the mixtures, at low temperature γ_φ exhibits relatively high values (1.118-3.032 N-sec/m^2) and thereafter decreases rapidly with increasing temperature. Applying the Arrhenius law to viscosity data [26], the activation energies (E_a) were calculated. In the mixtures **M1** to **M6** the E_a values are found to be 13.42, 14.65, 15.72, 19.22, 19.65 and 19.94 kJ/mol, respectively. Therefore, activation energy also increases with increasing concentration.

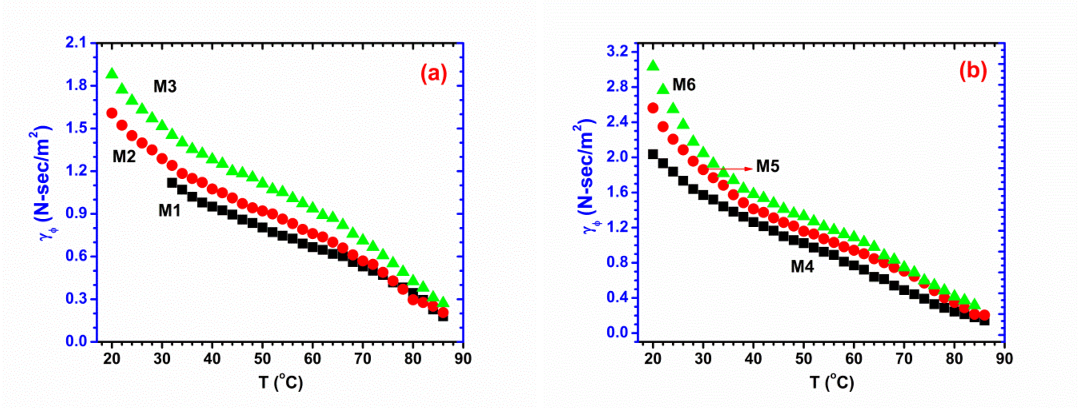

Fig. 11: Temperature variation of rotational viscosity (γ_φ): (a) **M1**, **M2**, **M3** and **(b) M4**, **M5,** and **M6**

For ease of comparison, various parameters important for display application have been listed in **Table 5**.

Table 5. Comparison of display parameters of the formulated mixtures at 20°C$^{\#}$

Mixture	T_{C*}-T_{A*} (°C)	ε'	P_S (nC/cm^2)	θ_{opt} (°)	τ (μs)	γ_φ (N-s/m^2)	E_a (kJ/mol)
M1	32-88	4.0	13	33.2	690	1.118	13.42
M2	<12-87.8	5.3	30	29.9	610	1.608	14.65
M3	<12-87.5	8.6	70	26.3	550	1.879	15.72
M4	<12-87.4	9.5	110	24.7	460	2.035	19.22
M5	<12-86.3	43.3	195	23.4	330	2.562	19.65
M6	<12-85.6	73.1	245	22.7	260	3.032	19.94

$^{\#}$parameters of **M1** at 32°C.

4. Conclusions

By varying concentration of a chiral terphenylate dopant into an achiral host matrix we have prepared six multi-component ferroelectric liquid crystal mixtures. Though the dopant is non-mesogenic in character, its mixtures in the multi-component host matrix exhibit a very wide range of ferroelectric SmC* phase starting from below room temperature, at least from 12°C. Various physical properties of the mixtures are found to be very sensitive to dopant concentration. With respect to the magnitude of different display parameters such as temperature range, dielectric permittivity, spontaneous polarization, optical tilt angle, rotational viscosity and response time the mixtures with moderate concentrations will be most suitable for SSFLC based applications.

Acknowledgments

We thankfully acknowledge the financial support under BRNS (DAE) project 2010/37P/44/BRNS/1441. Portions of this research were carried out at the light source PETRA III of DESY, a member of Helmholtz Association (HGF). Financial support by the Department of Science and Technology (Government of India) provided within the framework of the India@DESY collaboration is gratefully acknowledged. We are also grateful to Professor Roman Dabrowski, MUT, Poland for supplying the compounds.

References

[1] M. E. Lines and A. M. Glass. *“Principles and Applications of Ferroelectric and Related Materials”*. Oxford University Press, Oxford, 2001.

[2] L. Pardo and J. Ricote. *“Multifunctional Polycrystalline Ferroelectric Materials”*. Springer, Dordrecht, 2011.

[3] R. B. Meyer, L. Liebert, L. Strzelecki, et al. Ferroelectric Liquid Crystals. *Phys. Lett. (Paris)*. 1975; 36: 69-71.

[4] R. B. Meyer. Ferroelectric Liquid Crystals: A Review. *Mol. Cryst. Liq. Cryst.*, 1977; 40: 33-38.

[5] N. A. Clark and S. T. Lagerwall. Sub-microsecond bistable electro-optic switching in liquid crystals. *Appl Phys Lett.*, 1980; 36: 899-902.

[6] W. Kuczynski and H. Stegemeyer. Ferroelectric properties of smectic C liquid crystals with an induced helical structure. *Chem. Phys. Lett.*, 1980; 70: 123-126.

[7] M. Wand, R. Vobra, W. Thurmes, et al. New ferroelectric liquid crystal host materials for use in optoelectronic applications. *Proc SPIE*, 1994; 2175: 1-6.

[8] W. Thurmes, M. Wand, R. Vohra, et al. FLC materials form microdisplay applications. *Proc SPIE*, 1997; 3015: 1-6.

[9] M. Wand, W. Thurmes, M. Meadows, et al. FLC displays for high resolution magnified view and projection applications. *Proc SPIE*, 1999; 3635: 1-6.

[10] N. Bennis, A. Spadlo, R. Dabrowski, et al. Non-conventional alignment surfaces for antiferroelectric liquid crystals. *Mol. Cryst. Liq. Cryst.*, 2004; 422: 37-45.

[11] K Miyasato, S Abe, H Takezoe, et al. Direct Method with Triangular Waves for Measuring Spontaneous Polarization in Ferroelectric Liquid Crystals. *Jpn J App Phys.*, 1983; 22: L661-L663.

[12] P. G. de Gennes. "The *physics of liquid crystals*". oxford univ. press: Oxford, 1975.

[13] V. A. Baikalov, L. A. Beresnev, and L. M. Blinov. Measures of the molecular tilt angle and optical anisotropy n ferroelectric liquid crystals. Mol. *Cryst. Liq. Cryst.*, 1985; 127: 397-406.

[14] E. P. Pozhidaev, M. A. Osipov, V. Chigrinov, et al. Rotational viscosity of the smectic C* phase of ferroelectric liquid crystals. *Sov. Phys. JETP.*, 1988; 94: 125-132.

[15] I. Dierking. *Textures of liquid crystals*. WILEY-VCH: 2003.

[16] A. Debnath and P. K. Mandal. Effect of fluorination on the phase sequence, dielectric and electro-optical properties of ferroelectric and antiferroelectric mixtures. *Liq. Cryst.*, 44; 2017: 2192-2202.

[17] A. Debnath and P. K. Mandal. Dielectric properties of four room temperature ferroelectric and antiferroelectric multi-component liquid crystalline mixtures. *Liq. Cryst.*, Published online; 2017. doi: 10.1080/02678292.2018.1489986

[18] A. Debnath, D. Sinha, and P. K. Mandal. Wide range room temperature electroclinic liquid crystal mixture with large induced tilt and very small layer contraction. *J App. Phy.*, 119; 2016: 124103.

[19] A. Debnath, D. Sinha, P. K. Mandal, and R. Dabrowski. Formulation of a room temperature ferroelectric liquid crystal mixture with sub-millisecond switching time. *AIP Conf. Proc.*, 1665; 2015: 040004 (1-3).

[20] A. Debnath and P. K. Mandal. Wide range room temperature ferroelectric liquid crystal mixture with microsecond order switching. *J Mol. Liq.*, 221; 2016: 287-291.

[21] A. Debnath, P. K. Mandal, D. Węgłowska and R. Dabrowski. Induction of a room temperature ferroelectric SmC* phase in binary mixtures with moderate spontaneous polarization and sub-millisecond switching time. *RSC Advances*, 6; 2016: 84369-84378.

[22] M. Hird. Ferroelectricity in liquid crystals-materials, properties, and applications. *Liq. Cryst.*, 2011; 38: 1467-1493.

[23] J. Zubia, M. Castro, J. A. Puertolas, et al. Character of the smectic-*A*–chiral-smectic-*C* phase transition near a chiral-nematic–smectic-*A*–chiral-smectic-*C* point. *Phys. Rev. E.*, 1993; 48: 1970-1976.

[24] R. Bartolino, J. Doucet, and G. Durand. Molecular tilt in the smectic-C phase-zigzag model. *Ann. de Phys.*, 1978; 3: 389-395.

[25] M. S. Spector, P. A. Heiney, J. Naciri, et al. Electroclinic liquid crystals with large induced tilt angle and small layer contraction. *Phys. Rev. E.*, 2000; 61: 1579-1583.

[26] J. Hemine, C. Legrand, A. Daoudi, et al. Electro-optical and dielectric characterizations of the Goldstone mode relaxation in ferroelectric chiral smectic C liquid crystals. *J. Phys. Cond. Matt.*, 2007; 19: 296203(1-10).